Dynamic properties of supercooled Lennard-Jones liquids: a molecular-dynamics study

1990 J. Phys.: Condens. Matter 2 4991

(http://iopscience.iop.org/0953-8984/2/22/019)

J. Phys.: Condens. Matter **2** (1990) 4991–5003. Printed in the UK

Dynamic properties of supercooled Lennard-Jones liquids: a molecular-dynamics study

M J D Brakkee and S W de Leeuw
Laboratory for Physical Chemistry, University of Amsterdam, Nieuwe Achtergracht 127, 1018 WS Amsterdam, The Netherlands

Received 11 December 1989, in final form 14 March 1990

Abstract. Results are presented of molecular-dynamics experiments in which the Lennard-Jones liquid is cooled isobarically into the metastable temperature region. At a reduced temperature $T \simeq 0.45$ a specific-heat anomaly is observed. Results are given for the density and current-density correlation functions. The variation of viscosity and coefficient of self-diffusion with temperature can be fitted to a power-law behaviour with an exponent $\mu = 1.8$, in close agreement with predictions of recently proposed mode-coupling models.

1. Introduction

In the past few years, considerable theoretical and experimental attention has been paid to the area of the liquid–glass transition. In the domain of kinetic theories, much progress has been made, because these provide a mechanism for the glass transition and, at least in principle, incorporate a lot of phenomenological detail that can be compared with experimental observations. A number of models based on mode-coupling approximations have been proposed [1–6]. Some of the thermodynamic aspects of the liquid–glass transition, such as the changes in thermodynamic quantities across the glass transition, have been described within this framework [5].

On a rather general basis, work by Götze *et al* [4, 6] has supplied certain dynamic scaling laws that should hold for the dynamic structure factor of the undercooled liquid near the glass transition. Recent neutron scattering studies [7] seem to support these predictions.

However, it was found that the simpler mode-coupling models are valid only in a limited temperature region above the glass transition, and that close enough to the transition they break down. In later extensions, possible explanations have been given for this breakdown. Götze and Sjögren [6] introduced in their model equations a small regular contribution to the memory function of the density–density correlation function, which may model in a relatively simple way the non-ideality of real glass-formers and perhaps account for the observed differences between different classes of glasses. Das and Mazenko [8] started from a field theoretical approach, which allows a systematic handling of the couplings between the hydrodynamic fluctuations. They found that the non-linear feedback mechanism, which causes the sharp singularity in the simpler mode-coupling models, is still present but is cut off, which results in a rounded transition. All these theories, and especially later ones, have the drawback that numerical calculations

0953-8984/90/224991 + 13 $03.50

can only be performed for the simplest model systems and even then have to make crude simplifications, the consequences of which are hard to estimate. Calculations on the basis of a mode-coupling model by Bengtzelius *et al* [3] were carried through by the first for the Lennard-Jones (LJ) system [9].

This was one of the main reasons for us to take to computer simulations to test the results of theoretical predictions. Earlier work in this area was carried out by Fox and Andersen [10] and Ullo and Yip [11]. Although really long timescales cannot be probed by molecular dynamics (MD) techniques, MD simulations can still be useful because the onset of glass formation stretches over so many decades in timescale in a small temperature region. MD may also yield information about the kind of collective motions that remain accessible for the system at low temperatures. In this paper, we restrict ourselves to a presentation of our results on the thermodynamics and dynamics of the Lennard-Jones system in the supercooled region. In contrast to the work of Ullo and Yip, we consider explicitly the temperature variation of various quantities in the supercooled regime. Where possible, we shall compare our data with other experimental findings and theoretical predictions. Preliminary results of this work were presented in [12].

2. Molecular-dynamics experiment

The simulations were carried out for a system of 958 particles interacting through a Lennard-Jones (6, 12) potential, truncated at $r = 2.5\,\sigma$ and shifted to make it smooth at the cut-off radius. Throughout this paper, quantities are expressed in reduced units, as usual. We used Nosé's [13] constant-temperature and -pressure dynamics. In constant-temperature dynamics all degrees of freedom are coupled continuously in time to an external heat bath, and this allows one to cool the system in a way least distorting the evolution of the system. The constant-pressure method allows fluctuations in the volume of a MD cell. A fixed volume could be an unrealistic extra impediment for liquid-like relaxations, as Fox and Andersen pointed out [10]. For this reason we used the constant-pressure method. We did not observe the stress tensor to become significantly non-isotropic, so we believe there is no need for applying the general Parrinello–Rahman [14] dynamics.

We made slight modifications in Nosé's dynamics. Our extended system Hamiltonian for the isothermal–isobaric ensemble reads

$$H = \sum_i p_i^2/(2m_i V^{2/3} s^2) + \Phi(V^{1/3} q_i) + p_s^2/(2Q) + p_{ex} V$$
$$+ g k_B T \ln(s) + p_V^2/(2Ws^2) - k_B T \ln(V/V_0)$$
$$= H_0 + p_s^2/(2Q) + p_{ex} V + g k_B T \ln(s) + p_V^2/(2Ws^2) - k_B T \ln(V/V_0).$$

Here V is the volume of the system, Φ the potential energy, p_{ex} the externally applied pressure and s the time scaling parameter introduced by Nosé. The parameter s represents the coupling to a heat bath, and relative changes in s correspond to heat absorbed or given off by the bath. The q_i and p_i denote the scaled coordinates and momenta of the particles; p_V and p_s are the momenta conjugate to V and s respectively. Inertia is associated with both the parameter s and the volume motion: there are kinetic energy terms containing masses Q and W. The last term in our Hamiltonian is not present in the constant-pressure Hamiltonian originally proposed by Nosé. It is introduced to give the correct ensemble averages in the case where the total momentum is conserved, as in a MD system. V_0 is arbitrary, and it does not affect the equations of motion. More

important is the factor $1/s^2$ that we introduced in the kinetic energy term of the volume fluctuations. With this factor, all the equations of motion, including the equation of motion for the volume fluctuations, become scale-invariant (covariant) under a rescaling of the s parameter. This is as it should be, because the absolute value of the s parameter has no physical meaning, but only the relative change in s, this being proportional to the heat absorbed by the heat bath. Without this factor, one runs into problems with cooling simulations. During quenching, heat is being absorbed by the heat bath, and as a consequence the s parameter rises. This alone is sufficient to cause the volume fluctuations to become more and more rapid in real time. At a certain value of s, the volume fluctuations have become so rapid that the simulation is unstable and the system explodes. With this factor, the volume fluctuations have only a modest temperature dependence and the system behaves well down to the lowest temperatures used.

All simulations were carried out along the isobar of $p = 3.20\ \varepsilon/\sigma^3$. To reach a state in the supercooled liquid we always started at $T = 1.0\ \varepsilon/k_B$, where the liquid is stable, and subsequently cooled down the system. The runs were performed using a time step of about $0.004\ \tau$ (where $\tau^2 = m\sigma^2/\varepsilon$). We generated configurations in the undercooled liquid region in two ways: stepwise cooling and continuous cooling. In stepwise cooling, the system was repeatedly equilibrated for 10^3 time steps, simulated for 10^4 time steps and then instantaneously quenched over a fixed temperature interval of $0.1\ \varepsilon/k_B$. This means an average cooling rate of $2.2 \times 10^{-3}\ \varepsilon/k_B\tau$, which corresponds to $1.2 \times 10^{11}\ \mathrm{K\,s^{-1}}$ for argon. With this method, we did several quenches, starting from several independent configurations in the liquid. In continuous cooling, we separated cooling and production runs. A cooling run was performed by lowering the temperature by a fixed small percentage every time step. In this manner, the cooling rate was proportional to the temperature, and therefore higher at high temperatures where the system still can follow, and lower at low temperatures: about $9 \times 10^{-3}\ \varepsilon/k_B\tau$ on average. At several temperatures during such a quench, configurations were saved as starting configurations for subsequent production simulations. In general, we prefer the second method, mainly because of run-time economy. With this technique a single quench is sufficient for a low-temperature simulation, whereas with stepwise cooling a whole series of simulations at higher temperatures must be carried out.

Simulating a system that becomes increasingly non-ergodic near the glass transition means that one can no longer rely purely on time averaging. The way to overcome this problem is to repeat quenches, starting from 'independent' configurations in the liquid, and average over different quenches. Because time averaging becomes inefficient, there is really no need to extend simulations to longer times than necessary for attaining the desired time range of the time correlation functions.

An important problem and another reason for keeping simulations as short as possible must be discussed here. Bengtzelius *et al* [3] argued that, because in their mode-coupling model all correlations between more than four particles are wiped out of the equations, crystallisation, which requires complex particle rearrangements, is not present. This is not so in real systems, of course. The Lennard-Jones system in particular is a poor glass-former and quite unstable against crystallisation. For this reason, a great many of our simulations had to be discarded. To reduce the crystallisation probability we kept our simulations short. At first, we trusted any occurrence of crystallisation to develop in a relatively short time interval and to show up clearly as a sudden release of potential energy and a decrease in the cell's volume, and also as the appearance of crystalline peaks in the radial distribution function. This was also assumed by Fox and Andersen [10], and, in one particular MD study, observed by Hsu and Rahman [15].

Later on, this assumption proved to be too simple; crystallisation may indeed happen quite suddenly (with respect to the total simulation time) but it can also develop gradually in time. The critical nucleus may have formed before the crystalline peaks in $g(r)$ are visible [16]. Therefore, in addition to the signs already mentioned, we developed a method for checking on FCC crystallites in the real-space configuration and used a (at present heuristic) criterion to discriminate between 'good' and 'bad' configurations on the basis of this analysis. By only doing simulations starting with configurations in which FCC crystallites with size larger than a certain critical size were absent, we were able to increase the success rate of production runs (which meant quite a saving of computer time). One may question the meaning of the results obtained by such a selection procedure. We shall postpone that discussion to the last section of this paper. From this analysis, we found that below $T \leqslant 0.3$ in almost all cases the maximum crystallite size increased, regardless of the initial value. A similar observation was made by Honeycutt and Andersen [16] in their study of crystallisation of Lennard-Jones clusters. This means that below temperatures $T \simeq 0.3$ the system is unstable with respect to crystallisation.

3. Results

3.1. Thermodynamic quantities

We kept track of the volume and enthalpy during the simulations. As a function of temperature, these data follow a curve whose slope is everywhere almost constant except for a certain small temperature region where it changes smoothly, corresponding to a smoothed step in the respective temperature derivatives α_p and C_p. This feature is well known in experiments and is considered as marking the glass transision. To display this change in slope clearly we subtracted from our data a straight line with a slope approximately equal to the average of the slopes on both ends of the transition (see figure 1). With both continuous and stepwise cooling a cross-over from typical liquid-like to solid-like values of α_p and C_p was observed. Usually in experiments on glass-forming liquids this transition region is quite small and almost coincides with the iso-viscous glass transition temperature (often defined as that temperature where the shear viscosity $\eta = 10^{13}$ P). It is therefore not uncommon to associate the glass transition with this transition region. By fitting straight lines to both ends of the transition and determining their intersection, a glass transition temperature T_g is phenomenologically defined. Thus, from our data, $T_g \simeq 0.45\ \varepsilon/k_B$. At this temperature, the density is about $\rho = 0.98$. The transition region is quite broad, $\Delta T/T_g \simeq 0.2$. In recent experiments on organic glass [17] micrometre-sized droplets of the liquid were cooled at very high rates ($>10^5$ K s^{-1}). The step in C_p was observed at a much higher temperature than the isoviscous temperature T_g. Therefore, following the terminology of this paper, it is more correct to introduce another temperature, the fictive temperature T_f, to denote this transition point. It is called by that name because below this temperature the liquid is non-ergodic (within experimental timescales). One observes averages over a limited region of phase space, where the structure is identical to the liquid structure at T_f because structural relaxation does not occur within the duration of the experiment. For this reason, at T_f observed properties start to deviate from the metastable liquid curves below T_f. In these terms we find that in our simulations we observe a glass of fictive temperature $T_f \simeq 0.45\ \varepsilon/k_B$.

3.2. Dynamic quantities: single-particle properties

In all our simulations we calculated the mean-square displacement of the particles. We obtained the self-diffusion coefficient D from these data. Also, in one series of

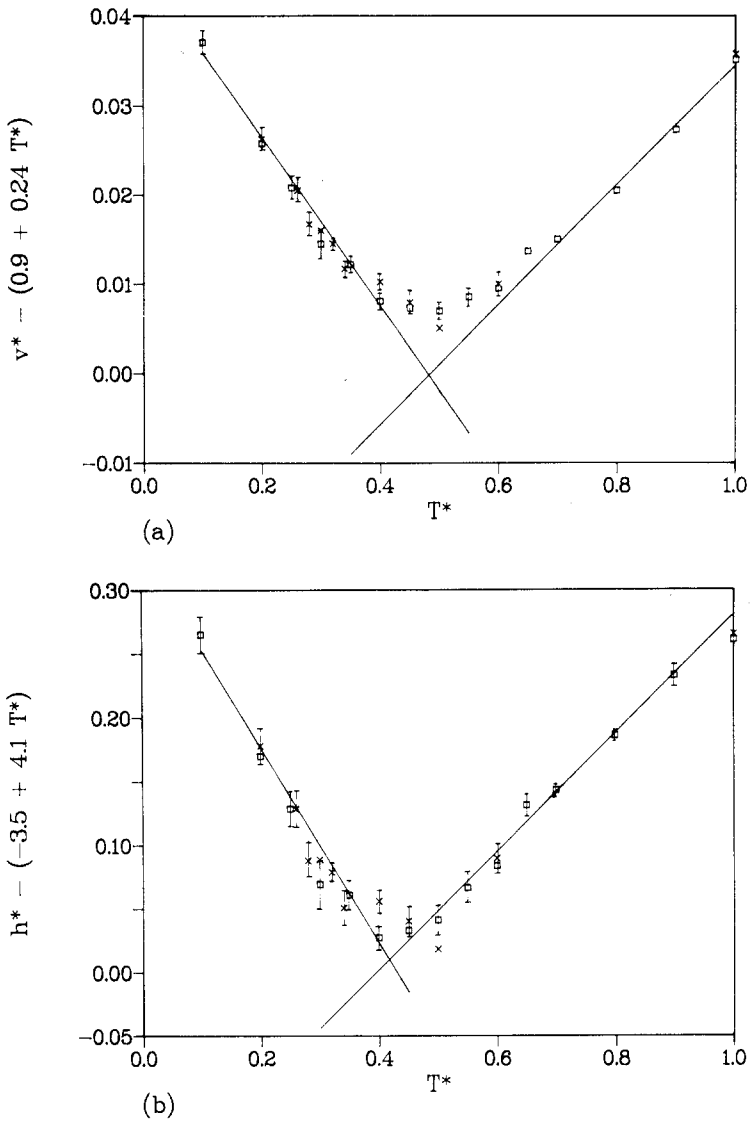

Figure 1. Temperature dependence of (*a*) the volume and (*b*) the enthalpy per particle. The average temperature dependence is subtracted to magnify the change in slope. The intersection of the two straight-line extensions determines the cross-over temperature T_f. Two cooling regimes: (□) stepwise cooling; (×) continuous cooling.

simulations, we calculated the self-intermediate scattering function $F_s(k, t)$. From these we extracted more accurate values for D by fitting to

$$\exp[-k^2Dt + E(t)k^4 - F(t)k^6 + \dots]$$

which is the asymptotic form of $F_s(k, t)$ in the case of normal particle diffusion. We used a few extra coefficients $E(t)$, $F(t)$, . . . , to allow for non-Gaussian effects in the limited time range of the simulation. The mode-coupling theories predict that the shear viscosity η is proportional to $(T - T_0)^{-\alpha}$ near the glass transition. If we assume that D remains approximately inversely proportional to η (or, more generally, $(d\eta/dT)$ (dD/dT) does

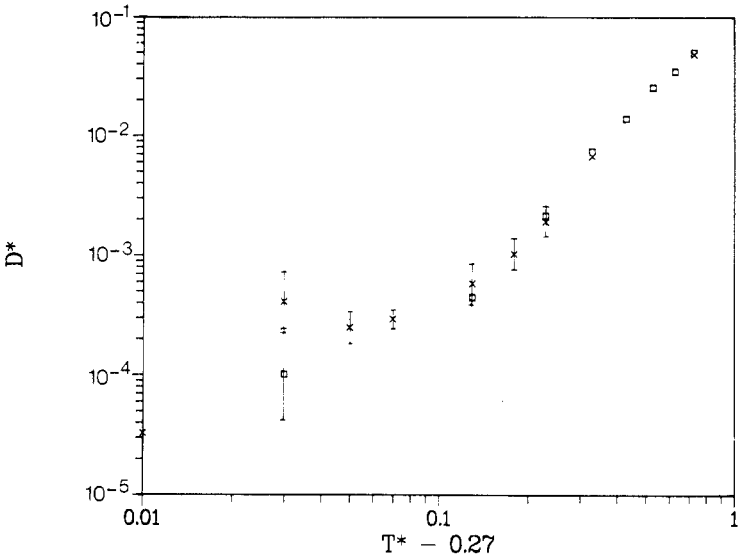

Figure 2. Diffusion coefficient $D/(\sigma^2/\tau)$, calculated in two ways: (□) obtained from the mean-square displacement of the stepwise cooling runs; (×) from self-intermediate scattering function of continuous cooling runs.

not diverge near the glass transition) a similar power law must also hold for D. In figure 2 our data are presented in a way to show this possible power-law dependence with $T_0 = 0.27$. In that case, $\alpha \simeq 1.8$, the fit is good for $T \geqslant 0.3\ \varepsilon/k_B$, below which temperature the data become more and more scattered and start to deviate. The value $\alpha = 1.8$ is typical of the theory, but the data may be fitted by a narrow but rather stretched out set of points in the (T_0, α) plane. The scattering of the data may be due to two effects. The first is increasing non-ergodicity, which means that time averaging becomes ineffective to sample contributions of all relevant phase space. This effect may be quite strong because of the limited size of the MD sample. The second effect is the instability of the liquid, which may cause some simulations to tend to crystallisation though it is not yet clearly visible in, for example, the radial distribution function. About $T = 0.3\ \varepsilon/k_B$ and below the data veer away from the power law; at T_0 we still measure finite values for D. This is entirely consistent with experimental observation that the shear viscosity follows a power law in a limited temperature region above T_0 and then crosses over to, possibly, Vogel–Fülcher or Arrhenius behaviour. Experimentally, T_0 is always found higher than T_g. If a viscosity of 10^{13} P (for argon) could be measured for this system, it would be at a temperature below T_0. We found $T_f > T_0$ and we cannot say anything about T_g. Theoretically, the status of an isoviscous T_g is of course problematic, for one thing because it does not scale according to the principle of corresponding states for LJ systems.

Often long-time tails in the glass transition region are described by a stretched exponential $\exp[-(t/\tau)^\beta]$ with β typically 0.5. The function $F_s(k, t)$ can be well fitted by this form for $t > 4\tau$. At high temperatures in the liquid we see no deviation of exponential decay. At lower temperatures, in some simulations the decay is clearly non-exponential. However, β is not sharply defined from these fits and the optimum values of β show no consistent picture as a function of temperature. Bengtzelius, in his calculations [9], found that in the intermediate time region $F(k, t)$ yielded a kind of separability law

$$F(k, t) \simeq a(k) \exp[-b(k)c(t)].$$

We tried to use this form for our $F_s(k, t)$ data, and it fits them well. We hoped that

in this way a $c(t)$ could be determined that has less statistical error than $F_s(k, t)$ for any individual k-value, but since the fluctuations for different k are strongly correlated, no accuracy is gained. In the case of normal diffusion, $c(t)$ is proportional to time and $b(k)$ sets off as k^2 for small k.

3.3. Dynamic quantities: collective properties

We calculated the following time autocorrelation functions:

$$F(k, t) = (1/N)\langle \rho_k(0)\rho_{-k}(t)\rangle$$
$$C_l(k, t) = (1/N)\langle j^l_k(0) j^l_{-k}(t)\rangle$$
$$C_t(k, t) = (1/N)\langle \boldsymbol{j}^t_k(0) \cdot \boldsymbol{j}^t_{-k}(t)\rangle$$
$$C_{KE}(k, t) = (1/N)\langle KE_k(0)KE_{-k}(t)\rangle$$

and

$$C_\sigma(t) = \langle \sigma^{xy}(0)\sigma^{xy}(t)\rangle.$$

Here ρ_k, j^l_k, $\boldsymbol{j}^t_k$, KE_k and σ^{xy} denote density, longitudinal current, transverse current, kinetic energy and the off-diagonal element of the stress tensor, respectively, according to

$$\rho_k(t) = \sum_j \exp[\mathrm{i}\boldsymbol{k} \cdot \boldsymbol{r}_j(t)]$$
$$j^l_k(t) = \sum_j \{\boldsymbol{k} \cdot \boldsymbol{v}_j(t)]/k^2\} \exp[\mathrm{i}\boldsymbol{k} \cdot \boldsymbol{r}_j(t)]$$
$$\boldsymbol{j}^t_k(t) = \sum_j \{\boldsymbol{k} \times [\boldsymbol{k} \times \boldsymbol{v}_j(t)]/k^2\} \exp[\mathrm{i}\boldsymbol{k} \cdot \boldsymbol{r}_j(t)]$$
$$KE_k(t) = \sum_j [v_j^2/(2m)] \exp[\mathrm{i}\boldsymbol{k} \cdot \boldsymbol{r}_j(t)]$$

and

$$\sigma^{xy}(t) = \sum_j [mv^x_j(t)v^y_j(t) + F^x_j(t)r^y_j(t)].$$

The most important of these functions is of course the intermediate scattering function $F(k, t)$. We plotted it for three different temperatures and three different k-values in figure 3. As the temperature is lowered, its relaxation can be described qualitatively as consisting of two parts, a fast relaxation due to vibrations, whose relaxation time does not change much, and a slow structural relaxation, whose relaxation time grows dramatically on lowering the temperature, due to structural arrest. This structural slowing down was also observed by Ullo and Yip [11]. It is strongly k-dependent, the structural arrest being most pronounced at wavenumbers corresponding to the position of the main peak in the static structure factor $S(k)$. This behaviour is reflected by the kinetic-energy correlation function, and at first sight it seems strange that it should do so, because one does not expect any divergence in the heat conductivity: heat should always flow about freely and not be obstructed by structural arrest. The explanation is that, though indeed kinetic energy is evenly spread out among the particles, it is always located on the particles and in this way its k-dependent correlation function reflects the structural slowing down. It is in fact straightforward to show that, for sufficiently large t,

$$C_{KE}(k, t) = \frac{1}{N}\left\langle \sum_{i,j} \frac{m^2}{4} v_i(0)^2 v_j(t)^2 \exp[\mathrm{i}\boldsymbol{k} \cdot \boldsymbol{r}_i(0)]\exp[-\mathrm{i}\boldsymbol{k} \cdot \boldsymbol{r}_j(t)]\right\rangle$$
$$\simeq (m^2/4)\langle v^2\rangle^2 F(k, t) = (3k_B T/2)^2 F(k, t)$$

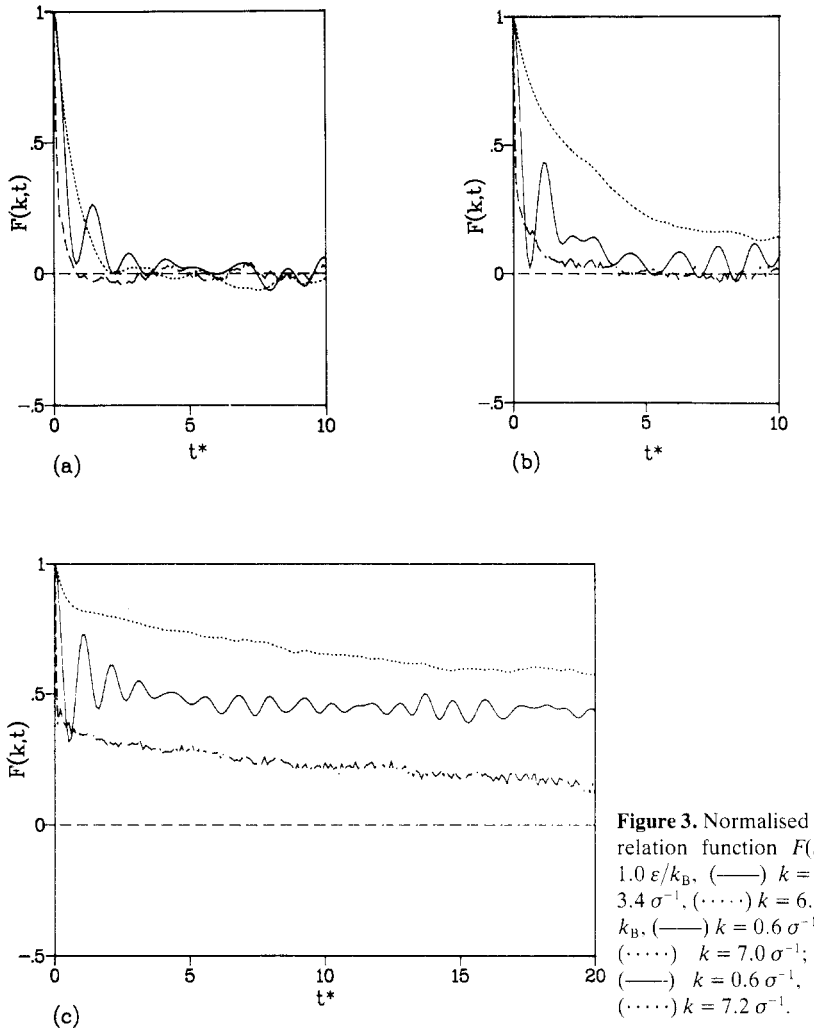

Figure 3. Normalised density–density correlation function $F(k, t)/S(k)$: (*a*) $T = 1.0\ \varepsilon/k_B$, (——) $k = 0.6\ \sigma^{-1}$, (– – –) $k = 3.4\ \sigma^{-1}$, (· · · · ·) $k = 6.8\ \sigma^{-1}$; (*b*) $T = 0.6\ \varepsilon/k_B$, (——) $k = 0.6\ \sigma^{-1}$, (– – –) $k = 3.5\ \sigma^{-1}$, (· · · · ·) $k = 7.0\ \sigma^{-1}$; (*c*) $T = 0.3\ \varepsilon/k_B$, (——) $k = 0.6\ \sigma^{-1}$, (– – –) $k = 3.6\ \sigma^{-1}$, (· · · · ·) $k = 7.2\ \sigma^{-1}$.

so the long-time tails in the kinetic-energy autocorrelation function are entirely determined by the density correlation. We tested this relation in our simulations and found that it is perfectly valid. Similarly, all wavevector-dependent correlation functions of any single-particle property with non-zero time average that for $t \to \infty$ has no autocorrelation and no cross-correlation with position may be expected to display the same long-time behaviour as $F(k, t)$.

In the dynamic theories, the important parameter is the so-called non-ergodicity parameter, the infinite-time limit of the normalised density correlation function,

$$f_k = \lim_{t \to \infty} F(k, t)/S(k)$$

because (in the idealised glass) it is singular across the glass transition, zero in the liquid and finite in the glass state. In reality, this singularity will only exist approximately, because eventually $F(k, t)$ will always go to zero because relaxation processes still occur in the glassy state, albeit at an extremely slow rate. Still, one may try to compare $F(k, t =$ large) with theory. Calculations based on mode- coupling approximations lead to a non-ergodicity parameter f_k that is similar in shape to $S(k)$ and with its main peak coinciding

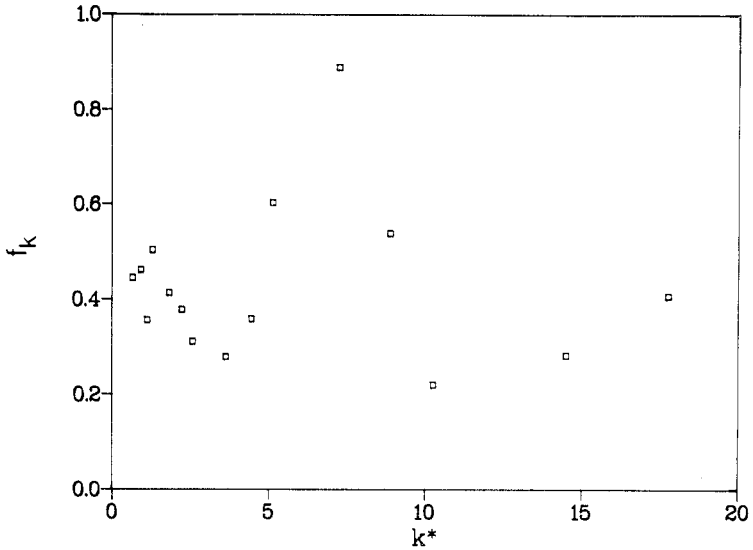

Figure 4. Plot of $f_k = F(k, t \simeq 20\,\tau)/S(k)$ for $T = 0.26\,\varepsilon/k_B$. The limited number of k-values cannot display all detail, but the peak at $7\,\sigma^{-1}$ is prominent.

with the main peak in $S(k)$. Figure 4, which shows $F(k, t = \text{large})$ for $T = 0.26$, demonstrates this clearly, and in this respect the mode-coupling approach seems to work.

The longitudinal current correlation function does not contain new information, as it is proportional to the second time derivative of $F(k, t)$. The transverse current correlation function does not have such a simple relation to $F(k, t)$. In a solid, transversely as well as longitudinally propagating density fluctuations exist. In a liquid, transverse sound may exist at short wavelengths, but vanishes for small enough k. However, as viscosity increases, the liquid becomes more and more solid-like and transverse sound appears at relatively long wavelengths and small frequencies, as can be seen in figure 5. At a certain temperature, the response is almost perfectly elastic; the $\omega = 0$ limit of the spectrum tends to zero.

The stress-tensor correlation function provides the route towards the shear viscosity through the Green–Kubo formula:

$$\eta = (\beta/V) \int_0^\infty \mathrm{d}t\, C_\sigma(t).$$

Of course, the (k, ω)-dependent shear viscosity may be determined from the transverse current correlation function, but, in an MD sample of limited size, extrapolation to the $\omega = 0$, $k = 0$ limit may be suspect. In figure 6, we plotted the normalised C_σ for three different temperatures, and its relaxation is clearly seen to become slower and slower. C_σ is very sensitive to instabilities in the system and contains a lot of noise. As long as it decays to zero within the duration of the simulation, η can be calculated reliably. When C_σ does not decay to zero within the simulation, one can still estimate η by assuming exponential decay, but of course, at low temperatures when there is very little relaxation, this will only give an indication of the order of magnitude. Our viscosity data, presented in figure 7, show a picture similar to our self-diffusion data: a power law, in agreement with mode-coupling predictions, is valid in a certain temperature region, but within experimental accuracy one cannot really discriminate between this behaviour and other, more traditional, functional forms for the temperature dependence of the viscosity.

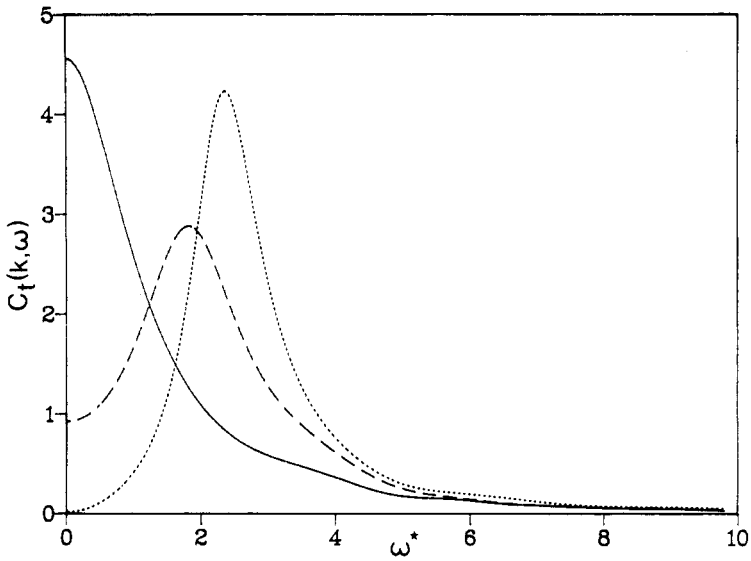

Figure 5. Spectrum of transverse current correlation function at $k \simeq 0.6\,\sigma^{-1}$: (——) $T = 1.0\,\varepsilon/k_B$; (– – –) $T = 0.6\,\varepsilon/k_B$; (· · · · ·) $T = 0.3\,\varepsilon/k_B$.

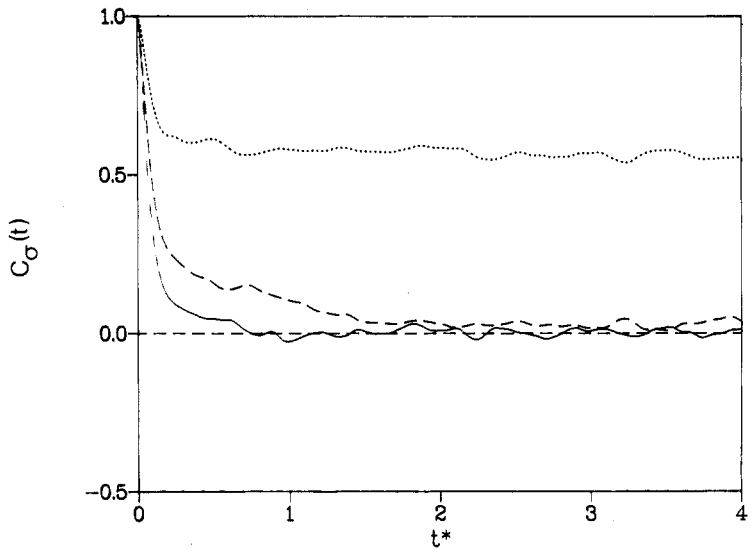

Figure 6. Normalised stress-tensor correlation function: (——) $T = 1.00\,\varepsilon/k_B$; (– – –) $T = 0.60\,\varepsilon/k_B$; (· · · ·) $T = 0.30\,\varepsilon/k_B$.

4. Discussion

In the temperature region $T > 0.3\,\varepsilon/k_B$ mode-coupling predictions work qualitatively well. Power-law behaviour of the shear viscosity, $\eta \propto |T - T_0|^{-\alpha}$, and of the self-diffusion coefficient, $D \propto |T - T_0|^{\alpha}$, with an exponent α of about 1.8, the theoretical value, is followed up to this temperature, if a T_0 of about $0.27\,\varepsilon/k_B$ is assumed. The value of T_0 lies well below the temperature T_f, where the anomalous behaviour in the specific

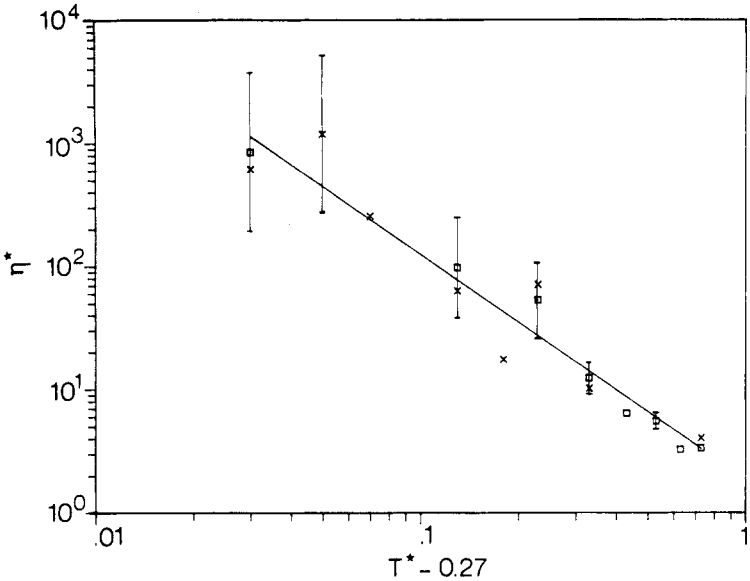

Figure 7. Viscosity $\eta/(\varepsilon\tau/\sigma^3)$ versus temperature: (□) stepwise cooling; (×) continuous cooling.

heat C_p and thermal expansion coefficient α_p is observed. This is what one would expect for experiments at a finite cooling rate if the transition is ideal, i.e. if the critical correlation time diverges at T_0: irrespective of the cooling rate the system leaves equilibrium at some temperature above T_0. In real systems relaxation times remain finite, and T_f may be found below T_0 provided one quenches slowly enough. Indeed, experimentally one usually observes T_0 to be well above T_f [18] and near T_f the temperature variation of the viscosity deviates strongly from the simple power-law behaviour predicted by mode-coupling theories. We attribute the reversed order of our T_f and T_0 with respect to what is found in real systems to the extremely high cooling rate in our simulations, which causes the supercooled liquid to leave equilibrium at temperatures well above the isoviscous glass transition temperature T_g. This has also been observed in rapid cooling experiments on microdroplets [17]. The limited accuracy of our data, especially below $T \simeq 0.45\,\varepsilon/k_B$, does not allow us to rule out other forms for this temperature dependence in favour of the mode-coupling form. Indeed, in real systems where η can be measured accurately over many decades, no universal relation has yet been found covering the viscosity behaviour over the whole temperature range of the supercooled liquid.

More positively, the simulations clearly reveal the importance of k_{max} = maximum of $S(k)$. The resemblance between the non-ergodicity parameter f_k and $S(k)$ is a natural consequence of mode-coupling theories, but should not be regarded as convincing evidence for its correctness. The observed resemblance may be quite trivial and not necessarily typical for the glassy state. Kinetic theory based on the Enskog generalisation of the Boltzmann equation predicts a significant minimum in the extended heat mode eigenvalue also at the maximum of $S(k)$ [19]. Quantitatively, Bengtzelius' calculations are quite a bit off, especially where the location of the glass transition line is concerned. One may argue that this is not very important, regarding the number of approximations that were made. It seems that the best we have is theory too complex to trust its numerical output, at least for the time being.

The Lennard-Jones system proves to be quite unstable against crystallisation below $T \simeq 0.3\,\varepsilon/k_B$. The region of phase space which contains glassy configurations that remain

stable during a sufficiently long time shrinks as the temperature is lowered. If it becomes so small that it includes only a small fraction of all phase space accessible by rapid quenching, one cannot speak about a glass any more: it is unstable against crystallisation. Up to $T \simeq 0.3\ \varepsilon/k_B$, one can view the Lennard-Jones system as a glass-forming system. Below this temperature, we observed that crystallisation becomes dominant.

One important conceptual question remains to be answered. If there is no singularity, what shall we mean by the glass transition? The definition of the glass transition temperature as that temperature where the shear viscosity attains a value of 10^{13} P is unsatisfactory from a theoretical point of view in two ways:

(i) The value of 10^{13} P is arbitrary.

(ii) The value of 10^{13} P does not scale. Our point is that if the glass transition should be characterised by a certain threshold viscosity, it should be a reduced threshold viscosity; something like the viscosity divided by the viscosity at the melting point.

We propose the following answer. The glass transition temperature is that temperature where the normal description of the liquid fails. The practical use of such a definition depends on what we consider the normal liquid description. The appearance of characteristic non-exponential relaxation occurs already in regions where the viscosity has only reached a value of 10 P or so. If we consider these effects as marking the glass transition, this definition would lead to a very wide glass transition region, and it would not be very practicable. But if these effects are well accounted for by mode-coupling theory, we might as well regard the mode-coupling description as normal liquid description, just for the reason that non-exponential relaxation effects are noticeable over a quite large region of temperature and pressure in the liquid phase, and not only close to the glass transition. Then we may characterise the liquid–glass transition by the breakdown of the mode-coupling description as in [1–5]. In practice, the breakdown may be identified as the point where the critical relaxation time ceases to follow the power-law divergence. Then the glass transition temperature lies slightly above the temperature where the relaxation time would diverge if the power law is extrapolated.

On a microscopic level, one may try to identify relaxation mechanisms that become dominant over the relaxation processes that determine structural relaxation on the liquid side of the glass transition. Of course, the problem is to analyse what the main modes of relaxation are. In particular, we note that dynamic processes of activated states are not yet included within the framework of mode-coupling models for the glass transition. It has been argued that such processes are of crucial importance for our understanding of the glass transition [20]. The study of such relaxations requires simulations on timescales much longer than presented here. This implies that better glass-forming models than the Lennard-Jones system must be investigated and that we need to study liquids at higher viscosities than in the present work. That is unfortunate, because such models necessarily will be more complicated and less amenable to theoretical analysis.

Since frustration is the cause of structural slowing down, and is effected by the repulsive part of the potential, and the detail of the molecular interaction and microscopic motion is of minor importance, a computer model may be looked for that still describes configurational effects well, but takes into account molecular motion only in a very simplified way. What may be found from computer models in order to improve on mode-coupling theories are those collective coordinates along which relaxation can take place when the simpler motions are frozen out.

Acknowledgments

This work is part of the research programme of the Foundation for Fundamental Research of Matter (FOM) and financially supported by the Netherlands Organisation

for Scientific Research. Some of the calculations were made possible by a grant of computer time by the Centre Européen de Calcul Atomique et Moléculaire (CECAM). We thank S Yip for useful discussions.

References

[1] Leutheusser E 1984 *Phys. Rev.* A **29** 2765
[2] Kirkpatrick T P 1985 *Phys. Rev.* A **31** 939
[3] Bengtzelius U, Götze W and Sjölander A 1984 *J. Phys. C: Solid State Phys.* **17** 5915
[4] Götze W 1985 *Z. Phys.* B **60** 195
[5] Bengtzelius U and Sjögren L 1986 *J. Chem. Phys.* **84** 1744
[6] Götze W and Sjögren L 1987 *Z. Phys.* B **65** 415
[7] Knaak W, Mezei F and Farago B 1988 *Europhys. Lett.* **7** 529
[8] Das S P and Mazenko G F 1986 *Phys. Rev.* A **34** 2265
[9] Bengtzelius U 1986 *Phys. Rev.* A **34** 5059
[10] Fox J R and Andersen H C 1984 *J. Phys. Chem.* **88** 4019
[11] Ullo J J and Yip S 1985 *Phys. Rev. Lett.* **54** 1509; 1989 *Phys. Rev.* A at press
[12] Brakkee M J D and de Leeuw S W 1989 *State and Dynamic Properties of Liquids (Springer Proc. Phys. 40)* p 154
[13] Nosé S 1984 *J. Chem. Phys.* **81** 511
[14] Parrinello M and Rahman A 1981 *J. Appl. Phys.* **52** 7182
[15] Hsu C S and Rahman A 1979 *J. Chem. Phys.* **70** 5234
[16] Honeycutt J D and Andersen H C 1987 *J. Phys. Chem.* **91** 4950
[17] Johari G P, Hallbrucker A and Mayer E 1989 *J. Phys. Chem.* **93** 2648
[18] Taborek P, Kleinman R N and Bishop D J 1986 *Phys. Rev.* B **34** 1835
[19] de Schepper I M, Haffmans A F E M and van Beijeren H 1986 *Phys. Rev. Lett.* **57** 1715
[20] Goldstein M 1969 *J. Chem. Phys.* **52** 3728